Development 133, 4643-4654 (2006) doi:10.1242/dev.02657

Shisa2 promotes the maturation of somitic precursors and transition to the segmental fate in *Xenopus* embryos

Takashi Nagano, Shoko Takehara, Maiko Takahashi, Shinichi Aizawa* and Akihito Yamamoto

In vertebrate somitogenesis, FGF and Wnt signals constitute a morphogenetic gradient that controls the maturation of the presomitic mesoderm (PSM) as well as the transition to segmental units. It remains unclear, however, whether there is a regulatory mechanism that promotes the transition by a direct regulation of FGF and Wnt signaling in the PSM. Here we show that Shisa2, a member of a novel Shisa gene family, plays an essential role in segmental patterning during *Xenopus* somitogenesis. *Shisa2* encodes an endoplasmic reticulum (ER) protein that cell-autonomously inhibits FGF and Wnt signaling by preventing the maturation and the cell-surface expression of their receptors. *Shisa2* is expressed in the PSM and its knockdown caused a reduction in somite number by the delayed maturation of PSM and anterior shift of the transition; however, the phase of the segmental clock remained intact. These phenotypes were abolished by the inhibition of both FGF and Wnt signals, but by neither alone. We therefore propose that the individual inhibition of both types of signaling by the regulation of receptor maturation in the ER plays an essential role in the establishment of proper segmental patterning.

KEY WORDS: Shisa, Somitogenesis, Wnt, FGF, *Xenopus*

INTRODUCTION

A metameric vertebrate body pattern is established by the segmentation of presomitic mesoderm (PSM), by which somites are formed sequentially along the anteroposterior (AP) direction at a regular interval. As a consequence of the maturation of unsegmented somitic precursors in the caudal PSM, cells have committed to a definitive segmental fate and form somitomeres, prospective somites, in the rostral PSM. A caudorostrally decreasing morphogenetic gradient (high caudally and low rostrally) distributes in the PSM; this gradient controls the maturation of PSM and the position in which cells transit to the definitive segmental fate (Aulehla and Herrmann, 2004; Dubrulle and Pourquie, 2004a; Saga and Takeda, 2001). This transition point, termed a 'wavefront', 'differentiation wavefront' or 'determination front' (Cooke and Zeeman, 1976; Dubrulle and Pourquie, 2004a), has been thought to be located at the border between the rostral and caudal PSM and marked by changes in the expression of two basic helix-loop-helix (bHLH) transcription factors. *Mesogenin1* (*Mes1*; *Xenopus* ortholog of *Mespo*) marks the caudal PSM (Joseph and Cassetta, 1999; Yoon et al., 2000; Yoon and Wold, 2000); *Thylacine1* (*Thy1*; *Xenopus* ortholog of *Mesp*) is expressed in two or three bilateral stripes that correspond to the anterior half of the somitomeres I-III (Fig. 3G) in the rostral PSM. The most posterior *Thy1* stripe in S-III is thought to represent PSM cells that have just passed the wavefront (Buchberger et al., 1998; Saga et al., 1997; Sawada et al., 2000; Sparrow et al., 1998). As somitogenesis proceeds, the wavefront moves posteriorly; this movement is tightly coupled with axial elongation.

A well-known signal constituting the gradient is FGF. The increase in the FGF/MAPK signaling suppresses the maturation of PSM cells and delays the transition to the segmental fate, consequently generating smaller somites. By contrast, the inhibition of FGF/MAPK signaling promotes the maturation of PSM cells and the generation of larger somites (Delfini et al., 2005; Dubrulle et al., 2001; Dubrulle and Pourquie, 2004b; Sawada et al., 2001).

The Wnt signal emitted from the tailbud has been implicated in the mechanism of the segmentation clock by which periodicity of segmentation is generated. In the mutant mouse harboring the *Wnt3a* hypomorphic allele *vestigial tail* (*vt*), expressions of several segmental clock genes are severely reduced or disrupted, including *Axin2*, Lunatic fringe, *Nkd1* and *Snail1* (*Snai1* – Mouse Genome Informatics) (Aulehla et al., 2003; Dale et al., 2006; Ishikawa et al., 2004). In the segmentation, increases and decreases in Wnt/β-catenin signaling generate smaller and larger somites, respectively, suggesting that Wnt signaling also functions as an inhibitor of the PSM maturation as FGF signaling does (Aulehla et al., 2003). It has thus been suggested that the wavefront is settled at the position where the level of FGF and Wnt signaling goes below a certain threshold (Aulehla and Herrmann, 2004; Dubrulle and Pourquie, 2004a). However, as the *FGF8* expression is strongly reduced in *vt/vt* mice, Wnt might set up the wavefront indirectly by regulating the FGF signaling (Aulehla and Herrmann, 2004). Thus it remains elusive whether individual regulation of both FGF and Wnt signals are required for the positioning of the wavefront.

The mechanisms establishing the PSM gradient have been explained in two ways. One is the axial elongation by which somitic precursors progressively move away from the tailbud, where cells actively transcribe and translate *FGF8* and *Wnt3a* genes. The decay and diffusion of the ligand protein regulate the gradient activity. Furthermore, as a result of a slow decay of *FGF8* transcripts, cells establish an *FGF8* mRNA gradient in the PSM; this mRNA gradient has been suggested to generate a shallow FGF8 protein gradient and to regulate the maturation of PSM (Dubrulle and Pourquie, 2004b). The other mechanism is the antagonistic relationship between retinoic acid (RA) and the FGF gradient. The RA signal constitutes a gradient that is rostrocaudally decreasing and has been suggested to promote the maturation of PSM. The increase and decrease in RA activity causes a posterior and anterior shift of the wavefront, respectively, through the indirect regulation of FGF signaling (Diez del Corral et al., 2003; Moreno and Kintner, 2004). By contrast to the

Laboratory for Vertebrate Body Plan, RIKEN Center for Developmental Biology, 2-2-3 Minatojima Minami, Chuo-ku, Kobe 650-0047, Japan.

*Author for correspondence (e-mail: saizawa@cdb.riken.jp)

Accepted 22 September 2006

gradient in extracellular ligands, however, it is largely unknown whether, and how, cells regulate their responsiveness to FGF and Wnt signaling for setting up the morphogenetic gradient in the PSM.

Wnts bind to the Frizzled (Fz) family of the seven-pass transmembrane receptor and activates a downstream target, Dishevelled. In the Wnt/β-catenin (canonical) pathway, this suppresses the activity of a protein kinase GSK3 (a negative regulator of this signaling), stabilizes β-catenin and activates transcriptional targets (Nusse, 2005). Wnt-Fz also initiates at least two other signaling cascades, planer cell polarity (PCP) and Wnt/Ca^{2+} pathway (Wallingford and Habas, 2005). In the early *Xenopus* embryos, integrations of this signaling govern numerous biological processes, including axis formation, convergent-extension cell movements, mesodermal differentiation and cell adhesion. FGF binds to the receptor tyrosine kinase FGF receptor family (FGFR1-4), and induces its dimerization and transphosphorylation. Subsequently, the small GTPase Ras transmits the FGFR signal and activates the protein kinase cascade Raf-MEK1/2-ERK1/2, which phosphorylates and activates various transcription factors (Goldfarb, 2001). FGF functions in the mesoderm and neural induction and their differentiation (De Robertis and Kuroda, 2004; Slack et al., 1996). We have recently reported isolation and functional characterization of Shisa1 (previously called Shisa) (Yamamoto et al., 2005), a cell-autonomous inhibitor for both Wnt and FGF signaling, involved in *Xenopus* head formation. Shisa physically interacts with an immature form of Fz and FGFR in the endoplasmic reticulum (ER) and inhibits their protein maturation and cell surface transportation, thereby suppressing events being initiated by ligand-receptor interactions of Wnt and FGF signaling.

Here we have identified Shisa-related genes in *Xenopus*, *Shisa2* and *Shisa3*, which inhibit both Wnt and FGF signals through the retention of their receptors in the ER as Shisa1 does. Knockdown study of Shisa2 suggests that it plays an essential role in the maturation of PSM cells by individual attenuation of both FGF and Wnt signaling.

MATERIALS AND METHODS

Embryonic manipulations

Animal cap, tailbud and dorsal explants were prepared at the stage indicated in the figure legends for each experiment. The explants were dissected in low-calcium magnesium Ringer's solution (LCMR) and cultured at 22°C with LCMR containing 0.1% bovine serum albumin (BSA) alone or with bFGF (50 ng/ml, R&D Systems), recombinant Human WIF1 (20 ng/ml, R&D Systems), mFz8CRD-Fc (30 ng/ml), SU5402 (0.1 mg/ml, CALBIOCHEM) or RA (1 μmol/l, CALBIOCHEM). mFz8CRD-Fc protein was prepared as described (Yamamoto et al., 2005). Morpholino antisense oligomers were obtained from Gene Tools: 5mis *Shisa2*MO1, 5′-GAGGCGTGCAACCACATCACTGGC-3′; *Shisa2*MO1, 5′-GAGCC-CTCCAACCACATGACTGGG-3′; *Shisa2*MO2, 5′-ACTCCTCTCACG-GGCAGCAAAAGTC-3′; 5mis *Shisa2*MO3, 5′-ACATGCCATTTATT-AGCTCCTCTAG-3′; *Shisa2*MO3, 5′-AGATCCCATTTATTACCTGCT-GTAG-3′. *Shisa1*MO was described previously (Yamamoto et al., 2005).

Cloning and construction of *Xenopus Shisa2* and *Shisa3*

The expressed sequence tag (EST) clone (Accession number CF286494: IMAGE 5516153) encoded a partial *Xenopus Shisa2* coding sequence (CDS), lacking 227 nt from the 3′ end of the CDS. To determine the full-length *Shisa2* cDNA sequence, 3′ RACE of the tadpole stage total RNA was carried out with a SMART RACE cDNA Amplification Kit (CLONTECH). The two forward primers 5′-GGTGGCAATTTGCTGTTGCAGATGT-3′ and 5′-AGTGCGAGCTGCGCTACTGCTGTT-3′ were used in a nested way. By the sequences of five independent clones, a full-length sequence of *Shisa2* cDNA was determined. The EST sequence of the BI449671 clone contained the full-length of *Shisa3* CDS. The CDS of *Shisa2* and *3* were amplified by RT-PCR and subcloned into *pCS2* (*Shisa2*/*pCS2* and *Shisa3*/*pCS2*). *Shisa2*-HA, *Shisa2*-Flag, *Shisa3*-HA and *Shisa3*-Flag were also generated by PCR. Other constructs were described previously (Yamamoto et al., 2005).

RT-PCR

RT reaction was carried out with MLTV (Invitrogen) using 500 ng of total RNA, isolated with RNA-STAT-60 (TEL-TEST Inc.) from embryos, animal caps or tailbud explants. PCR amplification was carried out for 28 cycles with the following thermal cycle profile: denaturation at 94°C for 30 seconds, annealing at 55°C for 45 seconds and extension at 68°C for 45 seconds, followed by a final extension at 72°C for 5 minutes. The primers used were: *Shisa2*, forward 5′-ACGATTCGACCATCTGCTG-3′ and reverse 5′-CAGTTGGTTTGGGATCGAGT-3′; *Mes1*, forward 5′-GAGA-CAACGGAGCTCTCACC-3′ and reverse 5′-AATCCAGCCTGGTGTT-TCAG-3′; *FGF8*, forward 5′-ACCTCCATCCTGGGCTATCT-3′ and reverse 5′-GCCCCTTCCATTAGTCTTCC-3′; *Wnt3a*, forward 5′-GC-GATTTTTGGACCAGTGTT-3′ and reverse 5′-TTCTGCCTGCTTCA-TTGTTG-3′; *Hes6*, forward 5′-GGCTGCTGATCTTCTGAACC-3′ and reverse 5′-CCTTCTCCCCTTCAGATTCC-3′; *Shisa2* F, 5′-ACGATTC-GACCATCTGCTG-3′; *Shisa2* R1, 5′-GAAATTCCATCATCCCAACC-3′; *Shisa2* R2, 5′-CAGTTGGTTTGGGATCGAGT-3′. Other primer sequences and conditions for PCR reaction were carried out as described previously (Yamamoto et al., 2005).

In situ hybridization, whole-mount immunostaining and western blotting

Whole-mount in situ hybridization was performed according to described procedure (Sive et al., 2000). Signals were developed with BM Purple (Roche) or BCIP (Roche). The probes used for in situ hybridization were transcribed from *Mes1*, XL322e02ex (NIBB); *Thy1*, XL220g19 (NIBB); *ESR9*, XL224g01ex (NIBB); *Arp-A*, XL146e16 (NIBB); *Cyp26*, XL322k18ex (NIBB); *Rarg*, XL275p11ex (NIBB); *Raldh2*, XL191i17 (NIBB); *Shisa2*, EXL1051-5991502 (Open Biosystems). *Xbra*, *MyoD*, *Papc* and *Wnt3a* were transcribed as described (Kim et al., 1998; Rupp and Weintraub, 1991; Smith et al., 1991; Wolda et al., 1993). *FGF8* cDNA was isolated by RT-PCR and cloned into the pGEMT-E vector (Promega). Western blotting was performed as described previously (Yamamoto et al., 2005). Antibodies against phospho-p44/42 MAP kinase (dp-ERK)(Cell Signaling), p44/42 MAP kinase (Cell Signaling) and HA (Covance) were used at 1:1000 dilution. Whole-mount immunostaining was performed according to described procedure (Kuroda et al., 2005).

Immunofluorescent staining, luciferase assay and co-immunoprecipitation assay

Immunofluorescent staining, luciferase assay and co-immunoprecipitation assay were carried out as described previously (Yamamoto et al., 2005). Cell transfection into COS cells was performed with Lipofectamine 2000 (Invitrogen), according to the manufacturer's instructions.

RESULTS

Identification of Shisa family members

Xenopus Shisa1 has two unique cysteine-rich domains (CRD1 and CRD2) in the amino-terminal half of the sequence (Fig. 1A) (Yamamoto et al., 2005). A search of a *Xenopus* EST database with the amino acid sequence of Shisa1 allowed us to identify two genes that encode Shisa family proteins harboring the two conserved CRDs (Fig. 1A,B); they are referred to as *Shisa2* and *Shisa3* (Accession number CF286494 for *Shisa2* and BI449671 for *Shisa3*). Among Shisa1, 2 and 3, the amino acid sequences are well conserved in the amino-terminal half, including the CRDs, but not in the carboxy-terminal half (Fig. 1C).

In the *Xenopus* animal cap assay, ectopic expression of Wnt8 or treatment with bFGF (FGF2) protein induces the expression of *Xnr3* and *Xbra*, respectively (Brannon et al., 1997; McKendry et al., 1997; Pownall et al., 1996). Shisa2 and 3 inhibited this induction in a dose-dependent manner, as Shisa1 does (Fig. 1D,E)

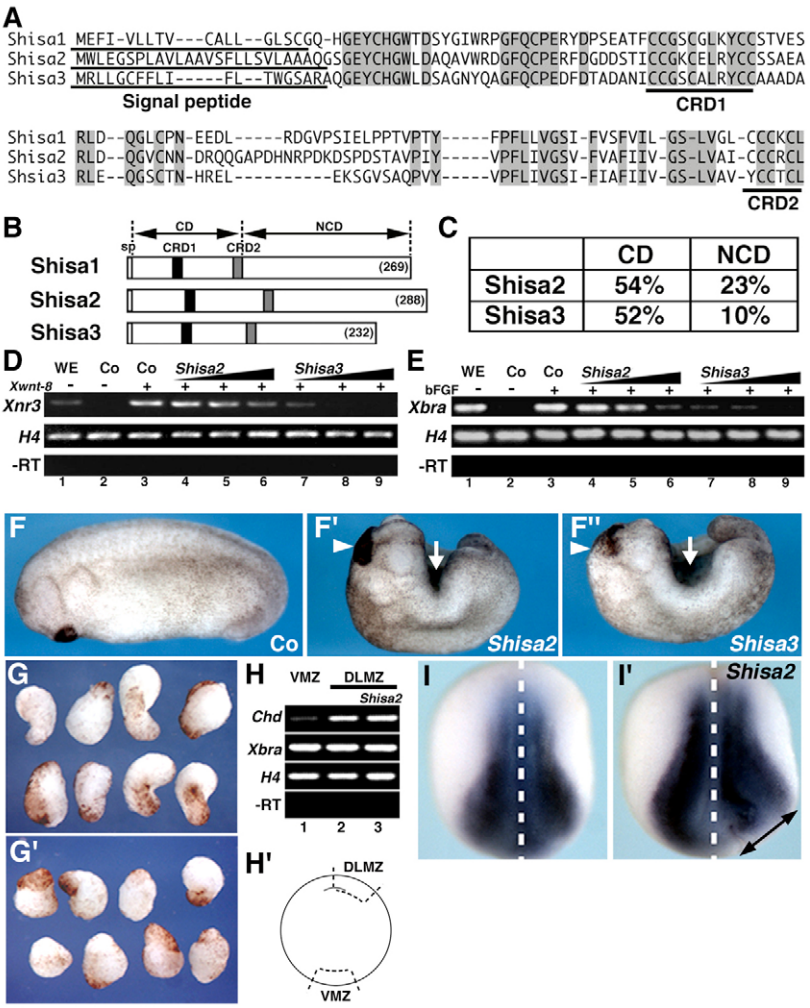

Fig. 1. Sequence comparison and biological activity of Shisa proteins. (**A**) Comparison of the predicted amino acid sequences of the conserved amino-half of the *Xenopus* Shisa family. Conserved amino acids are shown in gray. Cysteine-rich domains (CRD1 and 2) are underlined. Sequence analysis was carried out using GeneWorks. (**B**) Schematic protein structures of Shisa family members. Total amino acid lengths are presented in parentheses. (**C**) Identities of amino acid sequences (%) in the conserved domain and non-conserved domain of *Xenopus* Shisa family members with *Xenopus* Shisa1. (**D**) *XWnt8* (1 pg) RNA was injected either alone or together with *Shisa2* or *Shisa3* RNA (12.5 pg for lanes 4 and 7, 50 pg for lanes 5 and 8, 200 pg for lanes 6 and 9) into each animal blastomere at the eight-cell stage. RNAs were isolated from animal cap explants (AC) at late blastula and were analyzed by RT-PCR. (**E**) *Shisa2* or *Shisa3* RNA (100 pg for lanes 4 and 7, 200 pg for lanes 5 and 8, 400 pg for lanes 6 and 9) were injected into each animal blastomere at the four-cell stage. ACs were treated with or without bFGF for 3 hours and the expression of *Xbra* was analyzed as in D. (**F-F″**) Overexpression phenotype of *Shisa* genes. Radial injection of *Shisa2* RNA (F′) or *Shisa3* (F″) RNAs (50 pg) into the animal side of each blastomere at the four-cell stage. Resulting embryos had open neural folds (arrow) and enlarged cement glands (arrowhead) (*Shisa2*: 50%, *n*=30; *Shisa3*: 77%, *n*=34). (**G-H′**) Shisa2 inhibits the elongation of the dorsolateral marginal zone (DLMZ) explants. The DLMZ and ventral marginal zone (VMZ) explants (H′), were isolated at stage 10 and cultured until stage 12 (H) or stage 17 (G,G′). Explants from the normal embryos (G) or embryos injected with *Shisa2* RNA (3 pg per blastomere) at the four-cell stage (G′). (H) RT-PCR analysis of the DLMZ and VMZ explants. (**I,I′**) Whole-mount in situ hybridization of *MyoD* probe, dorsal view at neural stage. *Shisa2* RNA (3 pg) was unilaterally injected into two right side blastomeres at the four-cell stage (I′). (I) Uninjected embryo. Note that injection of *Shisa2* disturbed the convergence of the paraxial mesoderm on the injected side (double arrowhead) (*n*=16/28). CD, conserved domain; *Chd*: *Chordin*; Co, uninjected ACs; DLMZ, dorsolateral marginal zone; NCD, non-conserved domain; -RT, PCR with cDNAs synthesized without reverse transcriptase for *H4*; SP, signal peptide; VMZ, ventral marginal zone; WE, whole embryo.

(Yamamoto et al., 2005). Shisa2 and 3 neither induced neuroectoderm in animal caps or a secondary axis on the ventral side, nor did they inhibit Nodal/Activin-dependent *Mix2* expression (data not shown). These results indicate that Shisa2 and 3 uniquely inhibit Wnt and FGF signaling, but not Nodal/activin or BMP signaling.

To examine the overexpression phenotype of Shisa2 and 3, synthesized RNA was injected into four-cell stage embryos (Fig. 1F-F″). Embryos receiving a high dose of *Shisa2* or *Shisa3* RNA (50 pg per blastomere) exhibited a shortened body axis with an open neural tube (arrow) and enlarged cement gland (arrowhead), demonstrating that Shisa2 and 3 affect both AP patterning and morphogenetic activities of the *Xenopus* embryo. A low-dose injection of *Shisa2* (3 pg per blastomere) inhibited the elongation of the dorsolateral marginal zone explants of gastrulae without affecting the mesodermal differentiation (Fig. 1G-H′), showing that Shisa2 affects the convergent-extension cell movement of somitic precursors, possibly through regulation of the Wnt/PCP pathway. At the neurula stage, unilateral injection of a low dose of *Shisa2* RNA disturbed convergence of the *MyoD*-positive PSM cells toward the dorsal midline (Fig. 1I,I′).

Shisa2 and Shisa3 antagonize Wnt and FGF signaling by the retention of their receptors in the ER

Shisa2 and Shisa3 do not have a known ER retention signal, as is also true of Shisa1. In Hek293T cells, however, HA-tagged Shisa2 and Shisa3 specifically localized in the ER (Fig. 2A-B″). We examined the mode of action of Shisa2 and 3 in Wnt signaling in Hek293T cells. Ligand cells expressing Wnt3a and receptor cells expressing Fz8 and Lrp6 together with TOPFLASH reporter (Korinek et al., 1997) were prepared independently and mixed for stimulation. The non-cell-autonomous action of Wnt3a elevated the reporter activity (threefold; Fig. 2C, lane 2). When either Shisa 2 or 3 was coexpressed with Wnt-ligand, reporter activity was not affected (Fig. 2C, lanes 5 and 6); however, expression of Shisa2 or 3 in the receptor cells suppressed the reporter activity below the basal level (Fig. 2C, lanes 3 and 4), demonstrating that Shisa2 and 3 cell-autonomously inhibit Wnt signaling in these cells.

To analyze whether Shisa2 and 3 physically interact with Fz and FGFR, receptors tagged with HA were coexpressed together with Shisa2- or Shisa3-tagged Flag, and immunoprecipitated with anti-

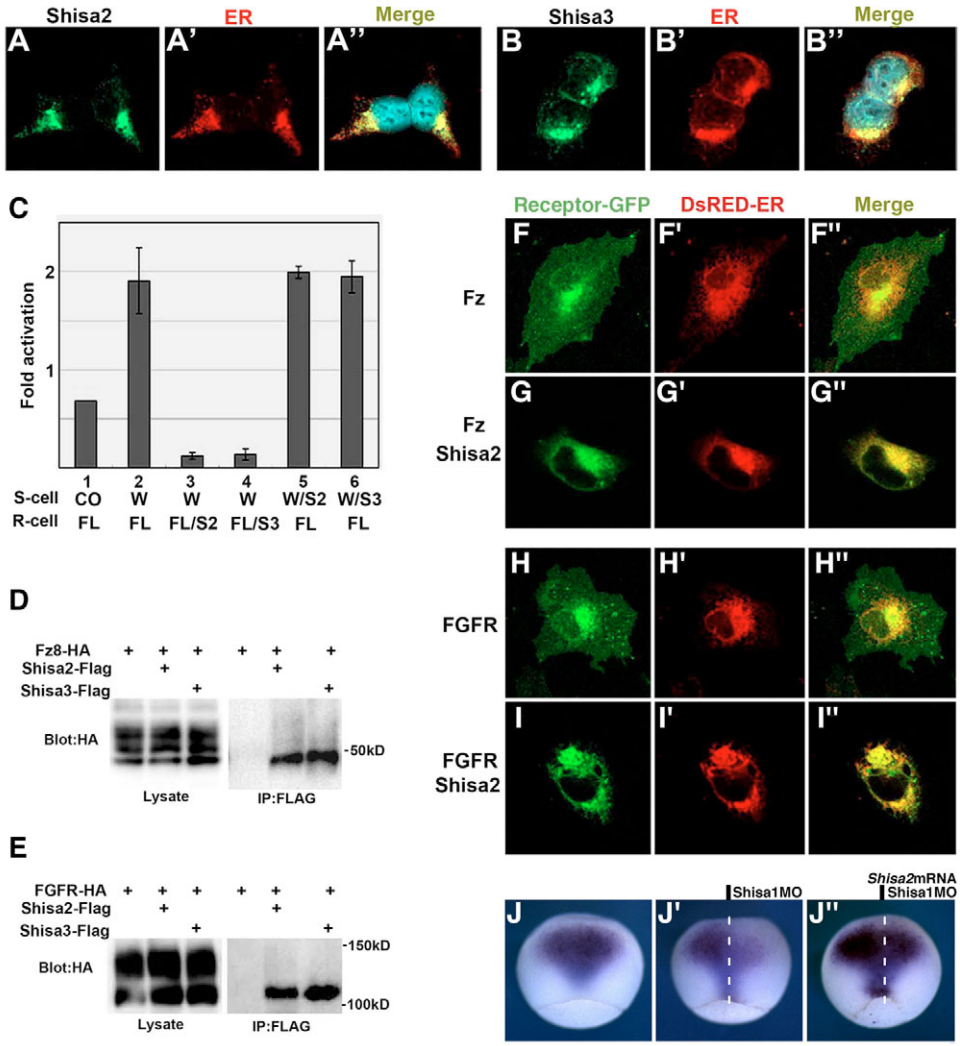

Fig. 2. The mode of molecular action of Shisa2 and 3. (**A-B″**) ER localization of Shisa2 and 3. HEK293T cells transfected with *Shisa2* (A) or *Shisa3*-HA (B) were stained for Shisa (green) and an ER marker calreticulin (red). Cells were transfected with 20 ng of *Shisa2* or *Shisa3*-HA DNA in a 96-well plate. (**C**) Shisa2 and 3 cell-autonomously suppressed the Wnt signal in the receptor cells. Ligand cells expressing Wnt3a (W) and receptor-cells expressing Fz and Lrp6 together with TOPFLASH reporter (F/L) were prepared independently and mixed for stimulation. The non-cell-autonomous action of Wnt3a elevated the reporter activity (threefold; lane 2). When either Shisa2 or 3 was coexpressed with the Wnt ligand, reporter activity was not affected (lanes 5, 6); however, expression of Shisa2 or 3 in the receptor cells suppressed the reporter activity below the basal level (lanes 3, 4). Each experiment was carried out at least in triplicate, and error bars represent the standard deviation. (**D**,**E**) Shisa2 and 3 physically interact with Fz (D) and FGFR (E). Fz- and FGFR-tagged HA were coexpressed together with Shisa2 or -3-tagged Flag, and immunoprecipitated with anti-Flag mAb. Cells were transfected in the 12-well plate with DNAs: *FGFR*-HA, 300 ng; *Fz8*-HA, 200 ng; *Shisa2*-Flag, 500 ng; *Shisa3*-Flag, 500 ng. (**F-I″**) Shisa2 and -3 retain the Fz and FGFR in the ER in COS cells. DsRedER marked ER. (F-F″) Transfected with *Fz8*-GFP alone (surface expression of Fz, *n*=24, 100%). (G-G″) Transfected with *Fz8*-GFP and *shisa2* (ER retention of Fz, *n*=21, 100%). (H-H″) Transfected with *FGFR*-GFP alone (surface expression of FGFR, *n*=20, 95%). (I-I″) Transfected with *FGFR*-GFP and *Shisa2* (ER retention of FGFR, *n*=22, 81%). Cells were transfected in 96-well glass chambers with DNAs: *Fz8*-GFP, 10 ng; *FGFR*-GFP, 20 ng; *Shisa2*, 180 ng; pDsRed-ER, 10 ng. (**J-J″**) Whole-mount in situ hybridization of *Otx2*, dorsal view at stage 10.5. *Shisa1*MO (10 ng) was unilaterally injected into two right side blastomeres at the four-cell stage. Reduced *Otx2* expression in the *Shisa1*MO injected side; *n*=28/40 (J′) and was rescued by co-injection of *Shisa2* RNA (10 pg per blastomere); *n*=32/42 (J″). (J) Uninjected embryo.

Flag mAb. We found the low molecular weight form of Fz8 and FGFR1 could be immature glycosylated Fz and FGFR (Yamamoto et al., 2005) in the precipitates of the Shisa2 and 3, indicating that Shisa2 and 3 physically interact with immature forms of Fz and FGFR (Fig. 2D,E). Furthermore, Shisa2 and 3 retain the Fz8 and FGFR1 in the ER (Fig. 2F-I″ for Shisa2; data not shown for Shisa3). We also examined whether Shisa2 retains other Fz homologs in the ER. In *Xenopus*, Fz2 and 7 are expressed in the PSM: they share 78% identities in the amino acid level (Deardorff and Klein, 1999; Sumanas et al., 2000). We found that Shisa2 retained Fz7 in the ER (*n*=20/20; data not shown). Altogether these results indicate that Shisa2 and 3 inhibit both Wnt and FGF signaling through the regulation of protein maturation and cell surface transportation of their receptors within the ER as Shisa1 does.

To further test the functional similarity of Shisa family members in vivo, we examined whether Shisa2 rescues the Shisa1 knockdown phenotype. Knockdown of Shisa1 suppressed the expression of *Otx2* at mid-gastrulation (Yamamoto et al., 2005). We found that injection of *Shisa2* RNA rescued this phenotype, suggesting that Shisa1 and 2 are functionally exchangeable in vivo at a molecular level (Fig. 2J-J″).

Expression of *Shisa2* in the *Xenopus* embryo

RT-PCR analysis showed that the *Shisa2* expression was weak throughout early embryogenesis and increased after the tailbud stage (Fig. 3A). Whole-mount in situ hybridization showed maternal and/or zygotic expression of *Shisa2* in the entire animal hemisphere by blastula stage (data not shown). *Shisa2* expression in the PSM was first detected at the beginning of neurulation (Fig. 3B). As somitogenesis proceeded, the *Shisa2* expression moved posteriorly (Fig. 3C), covering all the somitomeres (S-I, -II, -III) that have committed to segmentation and are visualized by *Thy1* expression (Fig. 3E,E′,G). The *Thy1* expression in the S-I and -II extended into the lateral plate mesoderm; however, *Shisa2* expression in this region was below the detectable level. In the caudal PSM, *Shisa2* showed a graded expression: high anteriorly

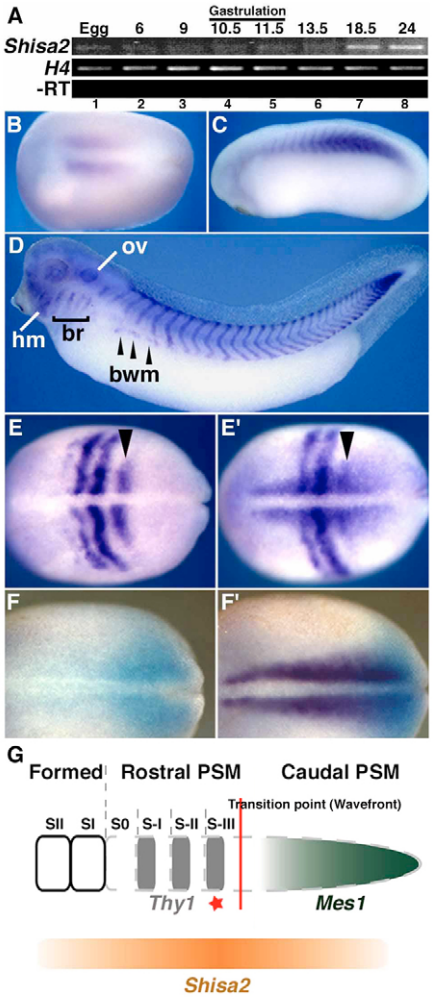

Fig. 3. Expression of *Shisa2* in somitogenesis. (**A**) Temporal expressions of *Shisa*2 were analyzed by RT-PCR with RNAs isolated from stages indicated at the top. (**B-F′**) Whole-mount in situ hybridization of *Shisa2*. (B) Dorsal view of the early neurula stage embryo (stage 14). Anterior is to the left. (C) Lateral view of tailbud stage embryo (stage 26). (D) Lateral view of tadpole (stage 33). (E-F′) Whole-mount in situ hybridization of stage 15 embryos (dorsal view, anterior towards the left). *Thy1* probe alone (E) or together with *Shisa2* probe (E′). *Shisa2* expression covers S-III/*Thy1* stripes (arrowheads in E and E′). *Mes1* probe alone (F, light blue) or together with *Shisa2* (F′, purple). *Shisa2* expression overlaps that of *Mes1*. (**G**) Schematic diagram showing the geometric relationship between the transition point and expression of *Thy1*, *Mes1* and *Shisa2*. The most caudal *Thy1* stripe marks the most newly fate-determined somitomere (S-III, red asterisk), which has just passed through the transition point (wavefront). bm, body wall muscle; hm, head mesenchyme; ov, otic vesicle.

and low posteriorly, extended laterally and partly overlapping with *Mes1* expression, a marker for the caudal PSM and tailbud (Fig. 3F,F′,G). At the tadpole stage, *Shisa2* expression was detected in the middle of each somite, precursors of the ventral body wall muscle, the otic and optic vesicles, head mesenchyme and brachial arches (Fig. 3D). We also found unique *Shisa3* expressions in ventral forebrain and ventral hindbrain at the tailbud stage (data not shown). Shisa3 might play a role in these tissues; however, this study focused on the role of Shisa2 in segmental patterning.

The role of Shisa2 in the establishment of segmental patterning

Two antisense morpholino oligonucleotides (MO) were generated toward the translation initiation site and 5′ untranslated region (UTR) of *Shisa2,* MO1 and MO2, respectively (Fig. 4A). MO1 and MO2 inhibited the translation of Shisa2, but not that of α-tubulin (Fig. 4B). In these studies, the MOs were unilaterally injected, the uninjected side serving as an internal control. During gastrulation, these MOs had no effect on the expression of *Xbra* (a pan-mesodermal marker) or *MyoD* (a myogenic marker), suggesting that Shisa2 has no role in mesoderm induction, or in the dorsoventral and anteroposterior patterning (Fig. 4C-D″). At the early neurula stage, the paraxial mesodermal region stained by *MyoD* expression was symmetrical in the MO-injected and uninjected side, suggesting that the early allocation of somitic precursors was not affected by the MO injection (Fig. 4E-E″).

In the early segmentation period (stage 18; in *Xenopus*, the first somite buds off at stage 16-17) (Hamilton, 1969), unilateral injection of MO1 and MO2 elicited the anterior shift of the expression of *Thy1* and *Papc* (Kim et al., 1998) for a distance of one to two segments; the level and the mediolateral width of their expression was not affected (Fig. 4F-G″). The anterior borders of *Mes1*, *Xbra*, *FGF8* and *Wnt3a* expressions in the caudal PSM and the tailbud were also expanded anteriorly in the *Shisa2*MO-injected side (Fig. 4H-K″). These results suggest that knockdown of Shisa2 causes delay of the maturation of PSM cells.

Although we tried to rescue the Shisa2 morphant phenotypes by co-injection of carefully titrated *Shisa2* RNAs, the morphogenetic defects of gastrulae caused by ectopic *Shisa2* expression severely disturbed early allocation of somitic precursors (as shown in Fig. 1F-I′): this made it difficult for us to come to any conclusion on this issue. To further confirm the specificity of the Shisa2 morphant phenotype, we generated a third *Shisa2*MO (MO3; Fig. 4A′), which inhibits splicing of endogenous *Shisa2* mRNA (Fig. 4B′). We found that unilateral injection of MO3 also resulted in the anterior shift of the expression of *Thy1* and *Mes1* (Fig. 4L-M′). These results further support the specificity of the Shisa2 morphant phenotypes.

Next we examined whether knockdown of Shisa2 caused anterior extension of Wnt and FGF signaling activities. In mice, *Axin2* has been thought to be a direct downstream target of Wnt3a in the PSM (Aulehla et al., 2003). In *Xenopus*, expression of the Axin-related gene (*Arp-A*) (Itoh et al., 2000) was also under the control of Wnt signaling but not FGF (see Fig. 8C-C″). In the Shisa2 morphant, the expression of *Arp-A* and phospho-ERK (dp-ERK) staining were extended anteriorly (Fig. 4N-O′), indicating that knockdown of Shisa2 caused anterior extension of both Wnt and FGF signaling activities. We also found the anterior extension of retinoic acid hydroxylase *Cyp26* (Hollemann et al., 1998) expression and RA receptor gamma *Rarg* (Pfeffer and De Robertis, 1994), but not that of a dehydrogenase of RA *Raldh2* (Chen et al., 2001) in the Shisa2 morphant (Fig. 4P,Q; data not shown for *Raldh2*).

Next we examined whether the depletion of Shisa2 affects the cyclic expression of the segmental clock gene. In *Xenopus*, three distinct phases of cyclic expression are observed for *ESR9* (*Hairy/Enhancer-of-split related 9*), a possible component in the Notch signaling cascade (Fig. 5A-C) (Li et al., 2003). By the Shisa2 depletion, the anterior border of the *ESR9* expression was expanded anteriorly; however, the phase of the expression was not affected (Fig. 5D-F for MO1; data not shown for MO2).

Histological analysis of the longitudinal horizontal section demonstrated that Shisa2 depletion elicited anterior displacement of the most newly formed somite for a distance of one to two somites,

accompanying the anterior expansion of PSM. The serial sections showed that the position of the first somite was symmetrically at the same level in the MO-injected and uninjected sides, and the segment number was reduced by the knockdown of Shisa2 (Fig. 5G-L). Our data suggest that the altered morphogenetic gradient by the Shisa2 deficiency affected the generation of somites for a few segments and consequently reduced their number.

Knockdown of Shisa2 inhibits delayed maturation of PSM elicited by the RA treatment and inhibition of FGF signaling

The maturation of PSM and transition to the segmental fate are known to be regulated by a morphogenetic gradient established by the interaction among RA, FGF and Wnt signaling. To address the role of Shisa2 in the setting up of the PSM gradient, we

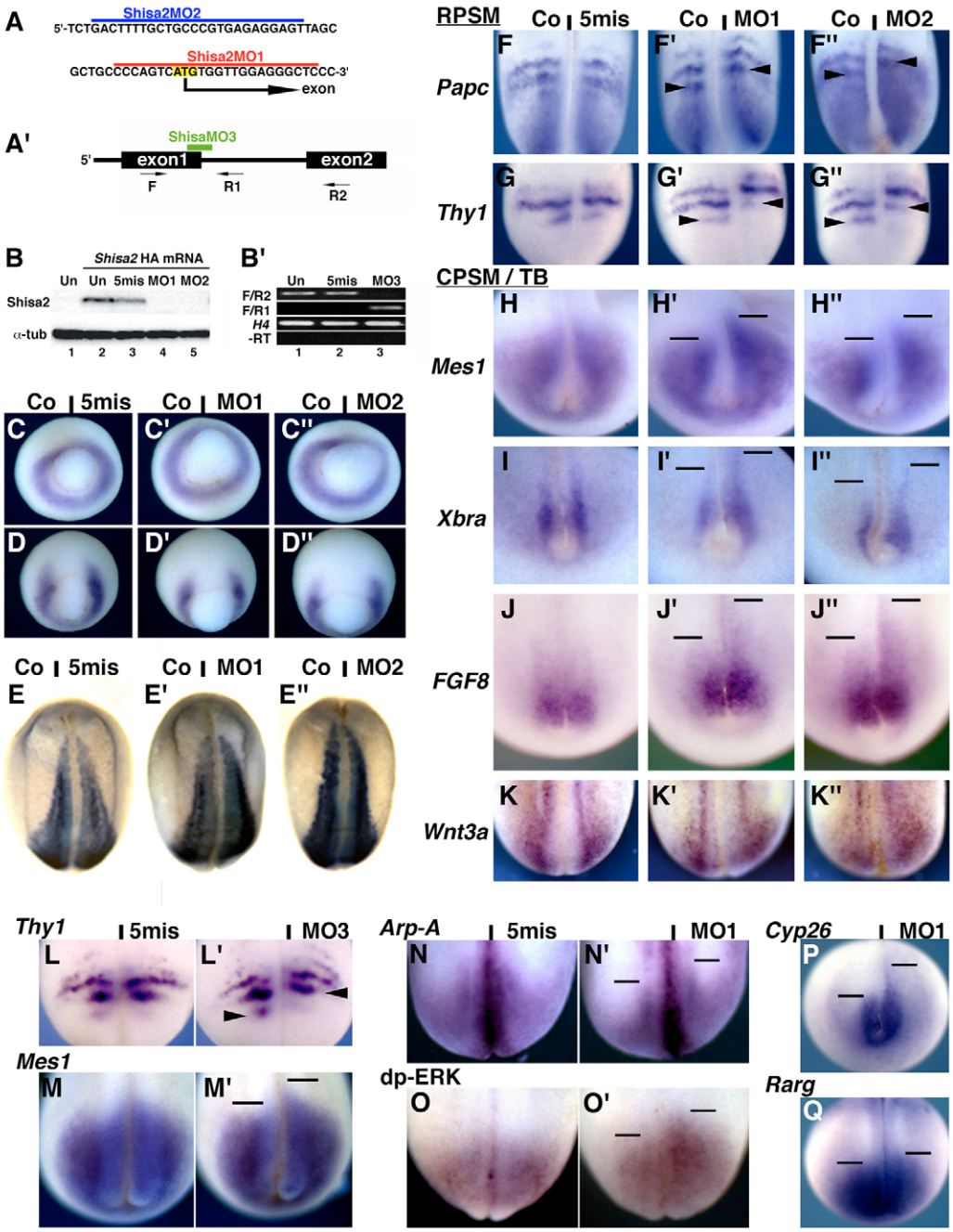

Fig. 4. Shisa2 controls the position of the wavefront. (**A**,**A′**) MO targeting *Shisa2* mRNA. (A) Sequences of *Shisa2*MO1 and MO2. (A′) MO3 was designed to block mRNA splicing. Immature and mature *Shisa2* mRNA was detected by RT-PCR using F/R1 and F/R2 primer set, respectively. (**B**) Four-cell stage embryos were injected with 50 pg of HA-tagged *Shisa2* RNA (lane 2) alone or together with *Shisa2*MOs (lane 3, 5mis, 40 ng per embryo; lane 4, MO1, 40 ng; lane 5, MO2, 20 ng). Lysate prepared from stage 10 embryos and probed with anti-HA antibody (upper panel) or anti-α-tubulin antibody (lower panel). (**B′**) Four-cell stage embryos were injected with 5mis-MO3 (lane 2, 30 ng per embryo) or MO3 (lane 3, 30 ng per embryo). Total RNA was isolated at stage18 and analyzed by RT-PCR. Note that MO3 injection inhibits splicing of *Shisa2* mRNA. (**C-Q**) Whole-mount in situ hybridization (C-N′,P,Q) or immunostaining (O,O′) of the embryos unilaterally injected with MOs (5misMO1, 10 ng; MO1, 10 ng; MO2, 5 ng; MO3, 7.5 ng; 5misMO3, 7.5 ng) into two right side blastomeres at the four-cell stage. (C-E″) MOs injection had no effect on *Xbra* (C-C″; 5mis, *n*=5/5; Mo1, *n*=15/15; Mo2, *n*=5/5) or *MyoD* (D-D″; 5mis, *n*=5/5; Mo1, *n*=12/12; Mo2, *n*=5/5) expressions at mid-gastrulation (stage 11). *MyoD* expression at early neurula (stage 18) was symmetrical in the MO-injected and uninjected side (E-E″; 5mis, *n*=15/15; Mo1, *n*=35/35; Mo2, *n*=21/21). (F-F″) Anterior shift of *Papc*; 5mis, *n*=0/17; MO1, *n*=44/59; MO2, *n*=21/21. (G-G″) Anterior shift of *Thy1*; 5mis, *n*=8/46; MO1, *n*=47/58; MO2, *n*=38/51. (H-H″) Anterior expansion of *Mes1*; 5mis, *n*=0/19; MO1, *n*=56/64; MO2, *n*=30/34. (I-I″) Anterior expansion of *Xbra*; 5mis, *n*=0/26; MO1, *n*=13/21; MO2, *n*=21/36. (J-J″) Anterior expansion of *FGF8*; 5mis, *n*=0/19; MO1, *n*=17/22; MO2, *n*=13/22. (K-K″) Anterior expansion of *Wnt3a*; 5mis, *n*=0/12; MO1, *n*=8/19; MO2, *n*=15/24. (L,L′) Anterior shift of *Thy1*; 5mis-MO3, *n*=0/30; MO3, *n*=18/36. (M,M′) Anterior expansion of *Mes1*; 5mis-MO3, *n*=0/20; MO3, *n*=17/30. (N,N′) Anterior extention of *Arp-A*; 5mis MO1, *n*=0/20; MO1, *n*=30/45. (O,O′) Anterior expansion of dp-ERK staining; 5mis MO1, *n*=0/11; MO1, *n*=12/19. (P) Anterior shift of *Cyp26*; MO1, *n*=11/29. (Q) Anterior shift of *Rarg*; MO1, *n*=10/21. Arrowheads represent S-II/*Papc* or S-III/*Thy1* stripes. Black bars indicate the anterior border of gene expressions or dp-ERK staining. CPSM/TB, caudal PSM and tailbud; RPSM, rostral PSM.

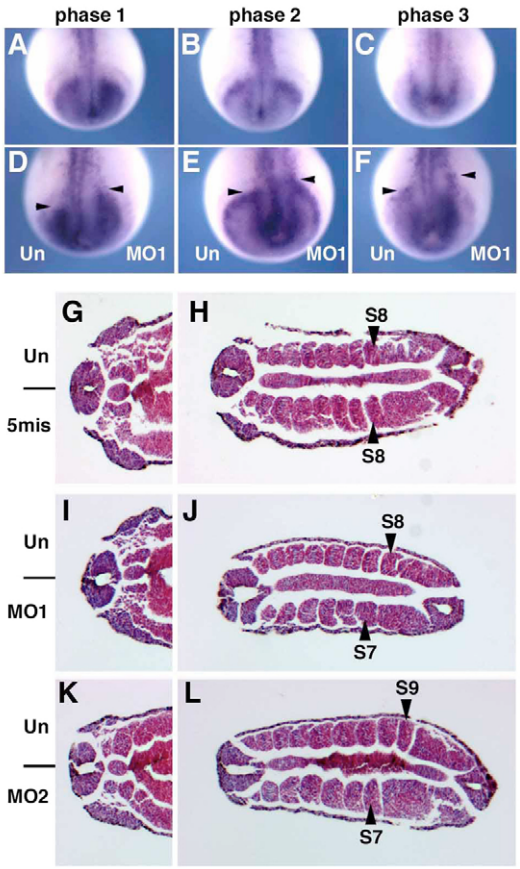

Fig. 5. Segmental clock and number of somites in Shisa2 morphants. Whole-mount in situ hybridization of wild-type embryos (**A-C**) or embryos unilaterally injected with MO1 (**D-F**) at stage 18 (posterior view, dorsal toward the top). The phase of cyclic *ESR9* expressions was determined according to Li et al. (Li et al., 2003). (A,D) Phase I. (B,E) Phase II. (C,F) Phase III. Arrowheads in D-F indicate the anterior border of *ESR9* expression. The phases of the *ESR9* expression between the MO-injected and uninjected side were symmetrical (5mis, *n*=14/17; MO1, *n*=24/24; MO2, *n*=25/29); however, the expression domain expanded anteriorly in the Shisa2-depleted side (5mis, *n*=0/19; MO1, *n*=18/24; MO2, *n*=22/29). (**G-L**) Longitudinal sections of the embryos unilaterally depleted Shisa2 stained with hematoxylene and eosin at the 6-9 somite stage. MO-injected sides are indicated on the left. (G,I,K) Sections of the level at the first somite. (H,J,L) Sections in a more posterior region of G, I and K. The positions of the last formed somites are displaced anteriorly in the Shisa2-depleted sides, for a distance of one (J; 5mis, *n*=2/11; MO1, *n*=10/16; MO2, *n*=6/15) or two (L; 5mis, *n*=0/11; MO1, *n*=2/16; MO2, *n*=4/15) somites.

examined the relationship between Shisa2 function and the RA/FGF gradient in the maturation of the PSM cells. Embryos unilaterally receiving *Shisa2*MO1 were treated with RA or SU5402 (a chemical inhibitor of FGFR function) at the early neurula stage for 1.5 hours, which approximately corresponded to the period in which two segments are generated (Hamilton, 1969), and then stained for *Mes1* and *Thy1* expressions. These treatments affect the maturation of the caudal PSM and the most newly formed segment in the S-III, but not older segments (e.g. S-I). In the uninjected side, both RA and SU5402 treatments abolished *Mes1* expression (Fig. 6A-C) and induced ectopic *Thy1* expression in the caudal PSM (Fig. 6D-F; ectopic *Thy1* expression is indicated by red arrowheads) (Moreno and Kintner, 2004). The treatments did not affect the endogenous *Shisa2* expression (Fig. 6J-J″). In the Shisa2-depleted side, both the reduction of *Mes1* expression and the ectopic induction of *Thy1* in the caudal PSM were significantly inhibited (Fig. 6A-F,G-I).

Although the knockdown of Shisa2 inhibited the effects of RA on the positioning of the S-III/*Thy1* stripe, it did not inhibit the RA-mediated expansion of *Thy1* expression (Fig. 6E; the expanded *Thy1* stripes are marked by white brackets), which is a direct target of RA signaling (Moreno and Kintner, 2004). RA treatment in wild-type embryos directly activated ubiquitous expression of *Cyp26* (Loudig et al., 2000) (Fig. 6K′). The knockdown of Shisa2 had no effect on the RA-induced *Cyp26* expression (Fig. 6K″). These results suggest that the inhibition of the effects of RA on the wavefront by the Shisa2 knockdown would be indirect.

In the tailbud explants, the depletion of Shisa2 also inhibited the reduction of *Mes1* expression by SU5402 treatment, the expression of *FGF8* and *Wnt3a* being unchanged (Fig. 6L). This Shisa2 knockdown effect was not caused by the reactivation of FGF signaling, as the SU5402 treatment strongly suppressed the activation of ERK/MAPK in both control and Shisa2-depleted embryos (Fig. 6M). These results strongly suggest that Shisa2 functions in the maturation of the PSM cells by regulating signals other than RA and FGF signaling, or by both FGF and Wnt signaling together.

Shisa2 promotes maturation of PSM cells through the inhibition of both Wnt and FGF signaling

As Shisa2 inhibits Wnt and FGF signaling, it is possible that inhibition of both these types of signaling canceled the anterior shift of the S-III/*Thy1* stripe in the Shisa2 morphants. To inhibit Wnt signaling, we injected a small amount of *Gsk3* RNA, an inhibitor of the canonical Wnt pathway but not of Wnt/PCP: this had no or little effect on the early allocation of PSM precursors at gastrulation (data not shown). Embryos radially receiving *Gsk3* RNA were subsequently injected with *Shisa2*MO1 unilaterally and were treated with SU5402 at the early neurula stage for 1.5 hours. This manipulation generated a larger posterior shift of the S-III/*Thy1* stripe in the Shisa2-depleted side and positioned the stripes in a symmetrical manner (Fig. 7A-A‴).

Next we further examined this issue using dorsal explants that were generated at the early neurula stage (stage 15) (Fig. 7B). The explants were treated for 1.5 hours with SU5402 and/or WIF1 protein, and subsequently analyzed for *Mes1* and *Thy1* expression. The knockdown of Shisa2 expanded *Mes1* expression anteriorly, as seen in the whole embryo (Fig. 7C). The inhibition of either Wnt or FGF signaling alone reduced *Mes1* expression in the uninjected side, whereas it was insufficient to abolish this expression in the Shisa2-depleted side (Fig. 7C′,C″). Inhibition of both types of signaling together, however, efficiently abolished *Mes1* expression in the caudal PSM of the Shisa2 morphants (Fig. 7C‴,F).

We then examined whether the inhibition of Wnt signaling by the WIF1 or conditioned media containing FzCRD (a soluble form of Fz8), together with SU5402 treatment, abolishes the anterior shifted S-III/*Thy1* stripe in the Shisa2 morphants. As in the case of *Mes1* expression, the inhibition of either signaling alone was insufficient to cancel the anterior shift of the stripe (Fig. 7D′,D″,E,G); however, inhibition of both types of signaling together positioned the stripe symmetrically (Fig. 7E′,E″,G). Altogether, the present results strongly suggest that Shisa2 promotes maturation of the PSM cells by the individual inhibition of both Wnt and FGF signaling.

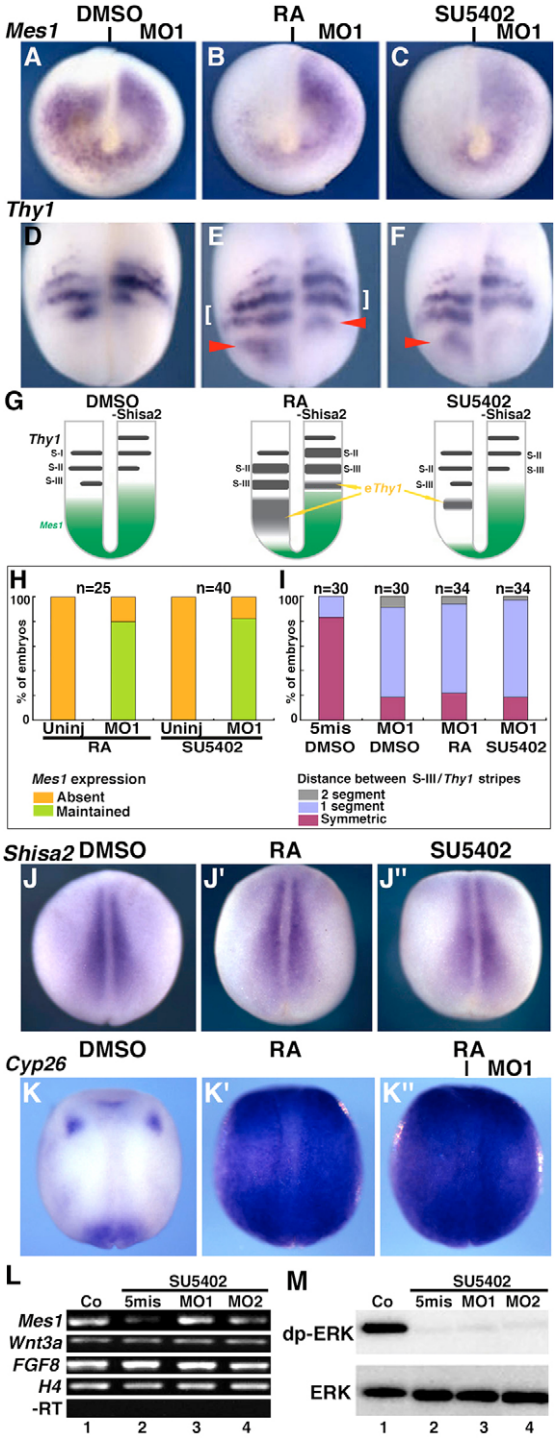

Fig. 6. Interaction of Shisa2 function and RA, Wnt and FGF signaling in the positioning of the wavefront. (**A-F**) Whole-mount in situ hybridization of *Mes1* probe (A-C, posterior view, dorsal toward the top) or *Thy1* probe (D-F, dorsal view, anterior toward the top). MO1 was injected as described in Fig. 4. At stage 14, embryos were treated with the indicated drug for 1.5 hours at 22°C and then fixed. (A,D) Embryos treated with DMSO. The unilateral depletion of Shisa2 resulted in the anterior expansion of *Mes1*, *n*=20/20, and anterior shift of *Thy1* stripes, *n*=24/30. (B,E) Embryos treated with RA. Knockdown of Shisa2 maintained *Mes1* expression (*n*=20/25) and suppressed the ectopic *Thy1* induction (*n*=28/34) in the caudal PSM. The arrowheads in E and F indicate ectopic *Thy1* expression. The RA-mediated enhancement of *Thy1* expression in the rostral PSM (white brackets in E) remained intact in the MO1-injected side (*n*=30/34). (C,F) Embryos treated with SU5402. Knockdown of Shisa2 maintained *Mes1* expression (*n*=32/40) and suppressed the ectopic *Thy1* induction in the caudal PSM (*n*=30/34). (**G**) Summary of the expression pattern of *Thy1* (gray) and *Mes1* (green) shown in A-F. e*Thy1*; ectopic *Thy1* expression in the caudal PSM. (**H**) Bar graph shows the effect of RA and SU5402 treatment on the *Mes1* expression. Abolished or maintained *Mes1* expression is indicated by an orange and green column, respectively. Uninj: uninjected side. (**I**) Bar graph shows the effect of RA and SU5402 treatment on the *Thy1* expression. The distance of S-III/*Thy1* stripe between the MO1-injected and uninjected side was evaluated as symmetrical (red), one somite distance (blue), two somite distance (gray). (**J-J″**) Whole-mount in situ hybridization of *Shisa2* probe. The endogenous *Shisa2* expression was unaffected by RA (J′) or SU5402 (J″) treatment. (**K-K″**) Whole-mount in situ hybridization of *Cyp26* probe. *Cyp26* expression was induced by RA (K′) and this induction was not inhibited by MO1 injection (K′). Ubiquitous expression of *Cyp26*; uninjected, *n*=30/30; MO1 injected *n*=32/32. (**L**) RT-PCR analysis of the tailbud explants treated with SU5402. Tailbud region was dissected at stage 15 from the control or embryos radially injected with *Shisa2*MOs (5mis and MO1, 40 ng per embryo; MO2, 20 ng per embryo) and cultured for 3 hours. SU5402 treatment was carried out for 1.5 hours at the end of the culture period. Note that SU5402 treatment reduced *Mes1* expression in the 5misMO-injected explants (lane 2) but in neither the MO1 nor MO2 explants (lanes 3, 4). (**M**) Western blot analysis of MAPK phosphorylation in whole embryos treated with SU5402 for 1.5 hours. *Shisa2*MOs were injected as described in J and treated with SU5402 for 1.5 hours from stage 14. MAPK phosphorylation was analyzed by anti-dp-ERK Ab (upper panel) and total MAPK by anti-ERK Ab (lower panel).

Positioning of the wavefront by Wnt and FGF signaling in the normal condition

The dorsal explants from wild-type embryos were treated with WIF1 or SU5402 for 1.5 or 3 hours. In the 3 hour treatment, but not in the 1.5 hour treatment, WIF1 and SU5402 suppressed MAPK phosphorylation and *Arp-A* expression, respectively (Fig. 8A-C″). These results show that the inhibition of each signaling for a longer period induces mutual regulation of their signaling activities.

To analyze the individual role in the positioning of the wavefront, we examined the average distance between S-II/*Thy1* and S-III stripes of the 1.5 hour explants. Compared with the SII-III distance of the control explants (*n*=36), that of SU5402-treated and WIF1-treated explants were 1.10-fold (*n*=51) and 1.15-fold (*n*=32), respectively (Fig. 8D-D″,E), suggesting that these two types of signaling individually reposition the S-III/*Thy1* stripes. We further asked whether the inhibition of these two types of signaling together synergistically reposition the wavefront posteriorly. The SII-III distance of the explants treated with WIF1 and SU5402 was 1.14-fold (*n*=34) (Fig. 8E). Thus we did not observe further posterior shift of the S-III stripe with the inhibition of both Wnt and FGF signaling together.

DISCUSSION

In a previous study we reported the characterization of Shisa1, which promotes *Xenopus* head formation (Yamamoto et al., 2005). Shisa1 uniquely inhibits Wnt and FGF signaling by suppressing the protein maturation of their receptors in the ER. It remains uncertain, however, whether this regulatory mechanism functions in other Wnt- and FGF-related events during vertebrate embryogenesis. To

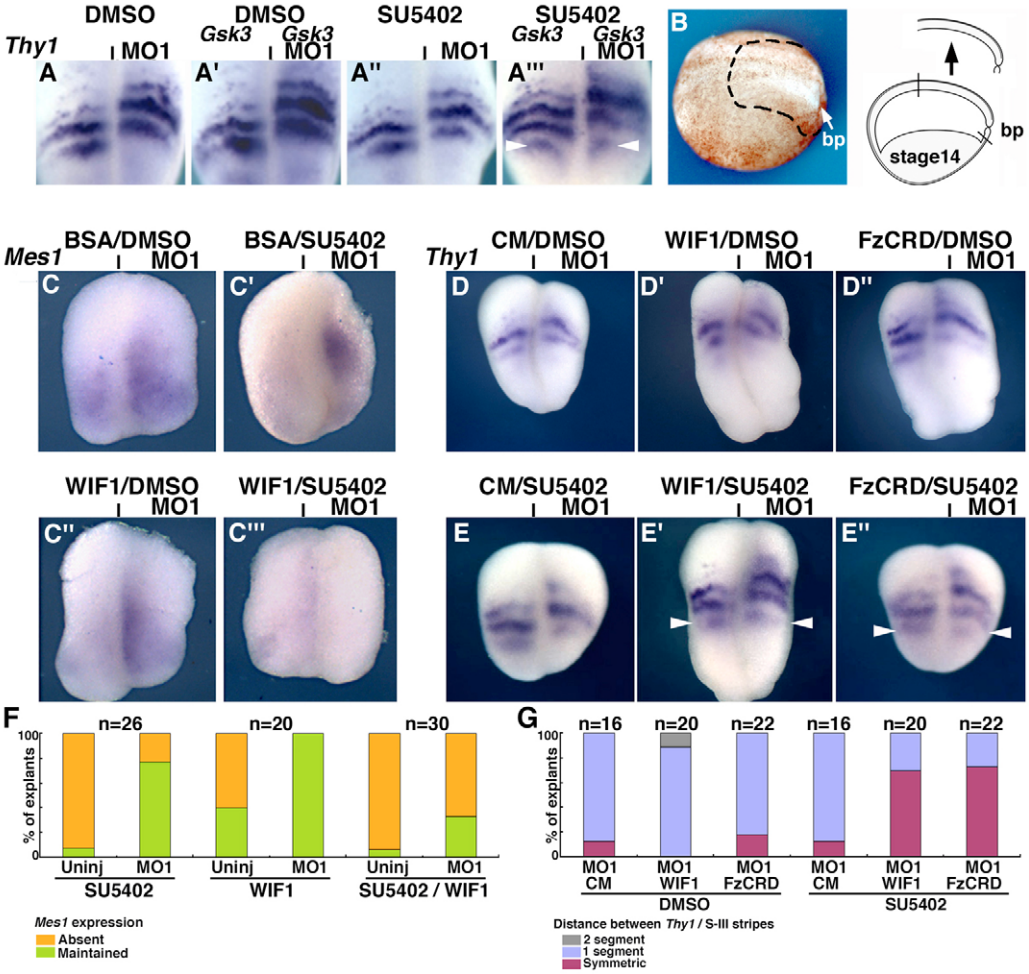

Fig. 7. Inhibition of Wnt and FGF signaling abolishes Shisa2 morphant phenotype. (**A-A‴**) Whole-mount in situ hybridization of *Thy1* probe (dorsal view, anterior toward the top). Two-cell stage embryos that had radially received *Gsk3* RNA (40 pg per embryo) (A′,A″) were subsequently injected with *Shisa2*MO1 unilaterally and were treated with DMSO or SU5402. Anterior shift of S-III/*Thy1* stripe in MO1-injected side; *Gsk3*/DMSO, 13/17; SU5402, 10/15, *Gsk3*/SU5402, 9/25. (**B**) Schematic diagram showing procedure of dorsal explant assay at stage 14. The dashed line on the left panel and the black bars on the right panel indicate the positions of cuts. bp: blastopore lip. (**C-C‴**) Whole-mount in situ hybridization of the dorsal explants with *Mes1* probe (dorsal view, anterior toward the top). The explants were generated from embryos unilaterally receiving MO1 at early neurulation (stage 14), treated with SU5402 and/or a recombinant WIF1 protein for 1.5 hours as indicated at the top, and then stained for *Mes1* expression. Abolished *Mes1* expression in the uninjected side; SU5402, 24/26; WIF1, 12/20; SU5402/WIF1, 27/30. Abolished *Mes1* expression in the MO1-injected side; SU5402, 6/26; WIF1, 0/20; SU5402/WIF1, 20/30. (**D-E″**) The dorsal explants from embryos unilaterally receiving MO1 were treated with SU5402 alone or together with Wnt inhibitors for 1.5 hours, and then stained for *Thy1*. The treatments are indicated at the top of each panel. Symmetric S-III/*Thy1* stripes (indicated by arrowheads in E′,E″) were observed in the explants treated with both FGF and Wnt signaling inhibitors but by neither alone (D′,D″,E). Anterior shift of S-III/*Thy1* stripe in MO1-injected side; BSA/DMSO, 14/16; BSA/SU5402, 14/16; WIF1/DMSO, 20/20; FzCRD/DMSO, 18/22; WIF1/SU5402, 6/20; FzCRD/SU5402, 6/22. Some explants were further cultured for 3 hours after WIF1/SU5402 treatment and fixed. Histological analysis showed the symmetric boundary formation in these explants (*n*=5/5). (**F**) Bar graph shows the effect of WIF1 and SU5402 treatment on the *Mes1* expression in the dorsal explants. Abolished and maintained *Mes1* expression is indicated with an orange and green column, respectively. (**G**) Bar graph shows the effect of WIF1, FzCRD and SU5402 treatment on the *Thy1* expression in the dorsal explants. The distance between S-III/*Thy1* stripe of MO1-injected side and that of uninfected side was evaluated as symmetrical (red), one somite distance (blue), two somite distance (gray).

address this issue, we isolated and characterized *Xenopus* Shisa-related genes, *Shisa2* and *3*. Our data indicate that Shisa-related molecules constitute a functionally conserved new gene family. Furthermore, we show that Shisa2-mediated regulation of FGF and Wnt signaling plays an essential role in segmental patterning during somitogenesis.

In segmentation, positional information provided by morphogenetic gradients controls the maturation of the somitic precursors and transition to the segmental fate. This crucial process takes place in the caudal PSM, where cells express the bHLH transcription factor *Mes1*, an essential factor for maintenance of the immature state of PSM as well as activation of the segmental clock (Yoon et al., 2000; Yoon and Wold, 2000). It seems likely that the termination of *Mes1* expression is a prerequisite to activate the expression of another bHLH transcription factor, *Thy1*, an essential factor for specifying a position of the segment boundary and the anteroposterior polarity of somites (Morimoto et al., 2005; Nomura-Kitabayashi et al., 2002; Saga et al., 1997; Sawada et al., 2000; Sparrow et al., 1998). It has recently been reported that *Mesp2* (mouse ortholog of *Thy1*) arrests the oscillation of Notch activity and initiates the segmentation program in the rostral PSM (Morimoto et al., 2005; Takahashi et al., 2000). Thus, the transition of the expression of these two transcription factors seems to be coincident with the wavefront. We found that both Wnt and FGF signaling are required in the initiation and/or maintenance of *Mes1* expression, and that the Shisa2-mediated inhibition of these two types of signaling is required for the proper termination of *Mes1* expression (Fig. 7). FGFR1, Fz7 and Fz2 are expressed in the PSM (Deardorff and Klein, 1999; Golub et al., 2000; Sumanas et al., 2000); Shisa2 would play an essential role in the regulation of the morphogenetic gradient by controlling protein maturation of these receptors. These present results provide an additional context, segmentation in the

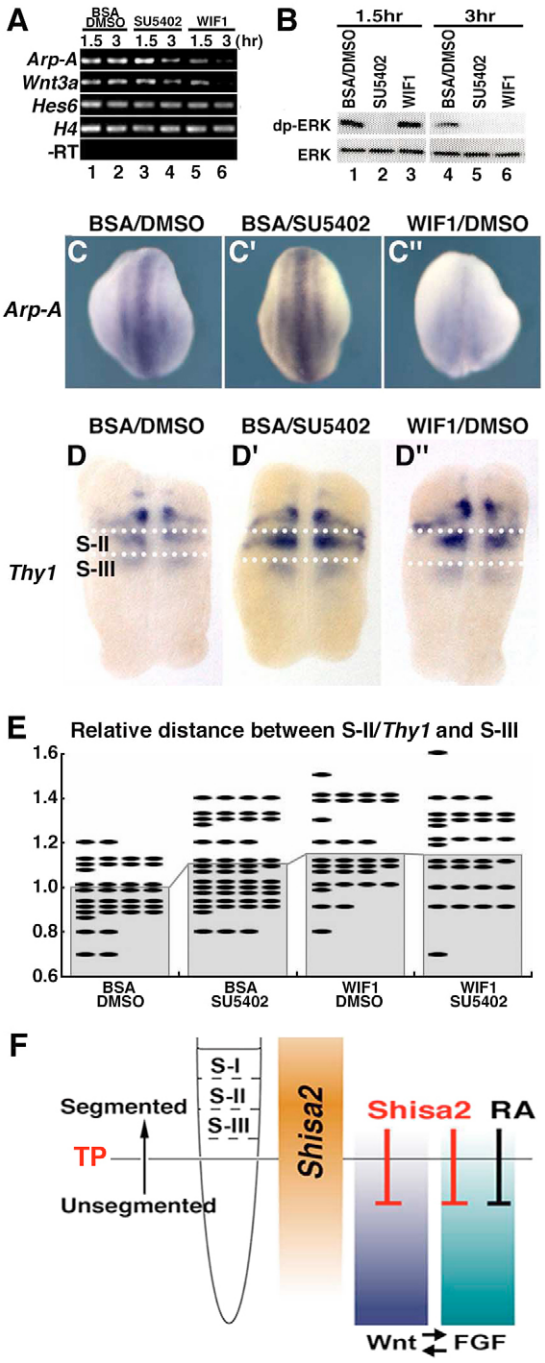

Fig. 8. Individual role of Wnt and FGF signaling in the positioning of the wavefront. (**A**) RT-PCR analysis of dorsal explants treated with SU5402 or WIF1. Dorsal explants were dissected at stage 14 from the normal embryos and cultured for 1.5 or 3 hours with 0.1% BSA in LCMR containing SU5402 or WIF1. (**B**) Western blot analysis of MAPK phosphorylation. The dorsal explants were treated with the indicated drug/protein for 1.5 or 3 hours. MAPK phosphorylation was analyzed by anti-dp-ERK Ab (upper panel) and total MAPK by anti-ERK Ab (lower panel). MAPK phosphorylation was reduced by 1.5-3 hours of SU5402 treatment (lanes 2, 5) or 3 hours of WIF1 treatment (lanes 3, 6). (**C-C″**) Whole-mount in situ hybridization of *Arp-A* probe. The dorsal explants were isolated from the neural stage normal embryos and treated with SU5402 (C′) or with WIF1 (C″) for 1.5 hours. Reduced *Arp-A* expression; BSA, 0/20; SU5402, 0/20; WIF1, 14/20. (**D-D″**) Whole-mount in situ hybridization of *Thy1* probe. The dorsal explants of the stage 14 normal embryos were treated with SU5402 (D′) or with WIF1 (D″) for 1.5 hours. Upper and lower dashed line indicates S-II/*Thy1* and S-III/*Thy1* stripes, respectively. (**E**) Bar graph shows the effect of SU5402, WIF1 and SU5402/WIF1 treatment on the relative distance between S-II/*Thy1* and S-III stripes. Gray bar and black dots indicate the average distance and individual distance, respectively. Data are represented as fold change, compared with the average distance of BSA/DMSO-treated explants (=1.0). (**F**) Summary of the role of Shisa2 in segmentation. The caudorostrally decreasing gradients of Wnt and FGF signal control the maturation of PSM and determine the position where cells transit to the definitive segmental fate (TP: transition point). *Shisa2* is expressed strongly in the region covering the TP, but its expression gradually decreases in the caudal PSM. Shisa2 positions the TP by the individual inhibition of the Wnt and FGF signaling. RA positions the TP at least in part by the indirect inhibition of FGF signaling.

PSM, in which Shisa-mediated signaling regulation controls cell-autonomous competence to respond to Wnt and FGF signaling for the establishment of vertebrate body patterning.

The role of Shisa2 in the establishment of the morphogenetic gradient

FGF8 and Wnt3a are expressed in the posteriormost mesoderm and generate signaling gradients: low rostorally and high caudally. Coupled with axial elongation during segmentation, diffusion of FGF8 and Wnt3a proteins, and also possibly decay of their transcripts, generates the morphogenetic gradient (Dubrulle and Pourquie, 2004b). We show, however, that in the absence of Shisa2 function, the regulation of FGF and Wnt ligands is not sufficient to generate the morphogenetic gradient for proper segmental patterning. Shisa2-mediated suppression of FGF and Wnt signaling in the PSM is required for setting up the gradient. *Shisa2* is expressed strongly in the region covering the wavefront, but its expression is low in the posteriormost PSM (Fig. 3). As somitogenesis proceeds, *Shisa2* expression moves posteriorly, coupled with axial elongation. Shisa2 inhibits surface expression of Fz and FGFR by retaining them in the ER. Thus, it is likely that Fz and FGFR are expressed at a high level in the posteriormost PSM and at a lower level in the anterior PSM. In this context, cells in the posterior PSM can respond to FGFs and Wnts better than those in the anterior PSM. In cooperating with the gradients of the ligand proteins, the gradients in the receptor expression may play a crucial role in setting up the morphogenetic gradient. As the knockdown of Shisa2 delays the maturation of PSM cells through the anterior extension of FGF and Wnt signaling activities, this mechanism would contribute to the formation of the morphogenetic gradient in the PSM.

In *Xenopus*, RA signaling is reported to inhibit FGF signaling by upregulating the MAPK phosphatase MKP3. A negative regulation of FGF signaling by RA is also reported in chick embryos (Diez del Corral et al., 2003; Moreno and Kintner, 2004). These reports suggest that RA signaling modifies the morphogenetic gradient at least in part by suppressing FGF signaling. Although the RA treatment or inhibition of FGFR caused a posterior shift of the wavefront (Moreno and Kintner, 2004) (Fig. 6), neither of them could suppress the phenotypes of the Shisa2 knockdown. The data indicate that inhibition of FGF by Shisa2 alone cannot explain the loss-of-function phenotype. The inhibition of both FGF and Wnt signals, however, strongly suppressed the phenotype and shifted the wavefront posteriorly (Fig. 7). Furthermore, in the normal condition

we found that the inhibition of these two types of signaling independently repositioned the third *Thy1* stripes posteriorly (Fig. 8). Altogether these results strongly suggest that Shisa2-mediated individual inhibition of Wnt and FGF signaling is required for the proper positioning of the wavefront.

The segmental clock in Shisa2-knockdown

The components of the Notch signaling cascade are involved in the segmental clock (Bessho and Kageyama, 2003; Giudicelli and Lewis, 2004; Pourquie, 2003; Rida et al., 2004). In *Xenopus*, the expression of *ESR9* and the closely related *ESR10* are oscillated in the caudal PSM (Li et al., 2003). We have found that the loss of function of Shisa2 expanded the anterior border of *ESR9* expression but did not affect its oscillation (Fig. 5). It has been suggested that FGF and Wnt signaling not only controls the maturation of the PSM and the position of the wavefront but also the segmental clock system. In *vt/vt* mutants, the expression of the cyclic genes is affected (Aulehla et al., 2003; Dale et al., 2006; Ishikawa et al., 2004). LEF/TCF factors, a component of the Wnt signaling cascade, directly control the expression of *Delta-like1*, thereby controlling the segmental clock (Galceran et al., 2004; Hofmann et al., 2004). In zebrafish, Her13.2 (Hes6-related hairy/Enhancer split-related), which functions downstream of FGF signaling, controls the expression of cyclic genes such as *Her1* and *Her7* (Kawamura et al., 2005). By contrast to these previous reports, Shisa2-mediated inhibition of FGF and Wnt signals did not affect the phase of expression of the *ESR9*. It is tempting to speculate that the high level of FGF and Wnt signals in the tailbud is the source of generation of the cyclic expression of the genes. Shisa2 controls the FGF and Wnt signals in the region more anterior to the tailbud; thus it controls the wavefront but not the segmental clock.

In summary, Shisa2 plays an essential role in the maturation of PSM and establishment of proper segmental patterning by the individual inhibition of Wnt and FGF signaling.

We thank the National Institute for Basic Biology of Japan for gifts of plasmids. We gratefully acknowledge Drs H. Takeda, Y. Saga, M. Hibi and M. Royle for helpful discussion and critical comments on this manuscript. This work was supported by Grants-in-Aid for Scientific Research on Priority Areas from the Ministry of Education, Culture, Sports, Science and Technology of Japan.

References

Aulehla, A. and Herrmann, B. G. (2004). Segmentation in vertebrates: clock and gradient finally joined. *Genes Dev.* **18**, 2060-2067.
Aulehla, A., Wehrle, C., Brand-Saberi, B., Kemler, R., Gossler, A., Kanzler, B. and Herrmann, B. G. (2003). Wnt3a plays a major role in the segmentation clock controlling somitogenesis. *Dev. Cell* **4**, 395-406.
Bessho, Y. and Kageyama, R. (2003). Oscillations, clocks and segmentation. *Curr. Opin. Genet. Dev.* **13**, 379-384.
Brannon, M., Gomperts, M., Sumoy, L., Moon, R. T. and Kimelman, D. (1997). A beta-catenin/XTcf-3 complex binds to the siamois promoter to regulate dorsal axis specification in Xenopus. *Genes Dev.* **11**, 2359-2370.
Buchberger, A., Seidl, K., Klein, C., Eberhardt, H. and Arnold, H. H. (1998). cMeso-1, a novel bHLH transcription factor, is involved in somite formation in chicken embryos. *Dev. Biol.* **199**, 201-215.
Chen, Y., Pollet, N., Niehrs, C. and Pieler, T. (2001). Increased XRALDH2 activity has a posteriorizing effect on the central nervous system of Xenopus embryos. *Mech. Dev.* **101**, 91-103.
Cooke, J. and Zeeman, E. C. (1976). A clock and wavefront model for control of the number of repeated structures during animal morphogenesis. *J. Theor. Biol.* **58**, 455-476.
Dale, J. K., Malapert, P., Chal, J., Vilhais-Neto, G., Maroto, M., Johnson, T., Jayasinghe, S., Trainor, P., Herrmann, B. and Pourquie, O. (2006). Oscillations of the snail genes in the presomitic mesoderm coordinate segmental patterning and morphogenesis in vertebrate somitogenesis. *Dev. Cell* **10**, 355-366.
Deardorff, M. A. and Klein, P. S. (1999). Xenopus frizzled-2 is expressed highly in the developing eye, otic vesicle and somites. *Mech. Dev.* **87**, 229-233.
Delfini, M. C., Dubrulle, J., Malapert, P., Chal, J. and Pourquie, O. (2005). Control of the segmentation process by graded MAPK/ERK activation in the chick embryo. *Proc. Natl. Acad. Sci. USA* **102**, 11343-11348.
De Robertis, E. M. and Kuroda, H. (2004). Dorsal-ventral patterning and neural induction in Xenopus embryos. *Annu. Rev. Cell Dev. Biol.* **20**, 285-308.
Diez del Corral, R., Olivera-Martinez, I., Goriely, A., Gale, E., Maden, M. and Storey, K. (2003). Opposing FGF and retinoid pathways control ventral neural pattern, neuronal differentiation, and segmentation during body axis extension. *Neuron* **40**, 65-79.
Dubrulle, J. and Pourquie, O. (2004a). Coupling segmentation to axis formation. *Development* **131**, 5783-5793.
Dubrulle, J. and Pourquie, O. (2004b). fgf8 mRNA decay establishes a gradient that couples axial elongation to patterning in the vertebrate embryo. *Nature* **427**, 419-422.
Dubrulle, J., McGrew, M. J. and Pourquie, O. (2001). FGF signaling controls somite boundary position and regulates segmentation clock control of spatiotemporal Hox gene activation. *Cell* **106**, 219-232.
Galceran, J., Sustmann, C., Hsu, S. C., Folberth, S. and Grosschedl, R. (2004). LEF1-mediated regulation of Delta-like1 links Wnt and Notch signaling in somitogenesis. *Genes Dev.* **18**, 2718-2723.
Giudicelli, F. and Lewis, J. (2004). The vertebrate segmentation clock. *Curr. Opin. Genet. Dev.* **14**, 407-414.
Goldfarb, M. (2001). Signaling by fibroblast growth factors: the inside story. *Sci. STKE* **106**, PE37.
Golub, R., Adelman, Z., Clementi, J., Weiss, R., Bonasera, J. and Servetnick, M. (2000). Evolutionarily conserved and divergent expression of members of the FGF receptor family among vertebrate embryos, as revealed by FGFR expression patterns in Xenopus. *Dev. Genes Evol.* **210**, 345-357.
Hamilton, L. (1969). The formation of somites in Xenopus. *J. Embryol. Exp. Morphol.* **22**, 253-264.
Hofmann, M., Schuster-Gossler, K., Watabe-Rudolph, M., Aulehla, A., Herrmann, B. G. and Gossler, A. (2004). WNT signaling, in synergy with T/TBX6, controls Notch signaling by regulating Dll1 expression in the presomitic mesoderm of mouse embryos. *Genes Dev.* **18**, 2712-2717.
Hollemann, T., Chen, Y., Grunz, H. and Pieler, T. (1998). Regionalized metabolic activity establishes boundaries of retinoic acid signalling. *EMBO J.* **17**, 7361-7372.
Ishikawa, A., Kitajima, S., Takahashi, Y., Kokubo, H., Kanno, J., Inoue, T. and Saga, Y. (2004). Mouse Nkd1, a Wnt antagonist, exhibits oscillatory gene expression in the PSM under the control of Notch signaling. *Mech. Dev.* **121**, 1443-1453.
Itoh, K., Antipova, A., Ratcliffe, M. J. and Sokol, S. (2000). Interaction of Dishevelled and Xenopus Axin-related protein is required for Wnt signal transduction. *Mol. Cell Biol.* **20**, 2228-2238.
Joseph, E. M. and Cassetta, L. A. (1999). Mespo: a novel basic helix-loop-helix gene expressed in the presomitic mesoderm and posterior tailbud of Xenopus embryos. *Mech. Dev.* **82**, 191-194.
Kawamura, A., Koshida, S., Hijikata, H., Sakaguchi, T., Kondoh, H. and Takada, S. (2005). Zebrafish hairy/enhancer of split protein links FGF signaling to cyclic gene expression in the periodic segmentation of somites. *Genes Dev.* **19**, 1156-1161.
Kim, S. H., Yamamoto, A., Bouwmeester, T., Agius, E. and De Robertis, E. M. (1998). The role of paraxial protocadherin in selective adhesion and cell movements of the mesoderm during Xenopus gastrulation. *Development* **125**, 4681-4690.
Korinek, V., Barker, N., Morin, P. J., van Wichen, D., de Weger, R., Kinzler, K. W., Vogelstein, B. and Clevers, H. (1997). Constitutive transcriptional activation by a beta-catenin-Tcf complex in APC–/– colon carcinoma. *Science* **275**, 1784-1787.
Kuroda, H., Fuentealba, L., Ikeda, A., Reversade, B. and De Robertis, E. M. (2005). Default neural induction: neuralization of dissociated Xenopus cells is mediated by Ras/MAPK activation. *Genes Dev.* **19**, 1022-1027.
Li, Y., Fenger, U., Niehrs, C. and Pollet, N. (2003). Cyclic expression of esr9 gene in Xenopus presomitic mesoderm. *Differentiation* **71**, 83-89.
Loudig, O., Babichuk, C., White, J., Abu-Abed, S., Mueller, C. and Petkovich, M. (2000). Cytochrome P450RAI(CYP26) promoter: a distinct composite retinoic acid response element underlies the complex regulation of retinoic acid metabolism. *Mol. Endocrinol.* **14**, 1483-1497.
McKendry, R., Hsu, S. C., Harland, R. M. and Grosschedl, R. (1997). LEF-1/TCF proteins mediate wnt-inducible transcription from the Xenopus nodal-related 3 promoter. *Dev. Biol.* **192**, 420-431.
Moreno, T. A. and Kintner, C. (2004). Regulation of segmental patterning by retinoic acid signaling during Xenopus somitogenesis. *Dev. Cell* **6**, 205-218.
Morimoto, M., Takahashi, Y., Endo, M. and Saga, Y. (2005). The Mesp2 transcription factor establishes segmental borders by suppressing Notch activity. *Nature* **435**, 354-359.
Nomura-Kitabayashi, A., Takahashi, Y., Kitajima, S., Inoue, T., Takeda, H. and Saga, Y. (2002). Hypomorphic Mesp allele distinguishes establishment of rostrocaudal polarity and segment border formation in somitogenesis. *Development* **129**, 2473-2481.
Nusse, R. (2005). Cell biology: relays at the membrane. *Nature* **438**, 747-749.
Pfeffer, P. L. and De Robertis, E. M. (1994). Regional specificity of RAR gamma isoforms in Xenopus development. *Mech. Dev.* **45**, 147-153.

Pourquie, O. (2003). The segmentation clock: converting embryonic time into spatial pattern. *Science* **301**, 328-330.
Pownall, M. E., Tucker, A. S., Slack, J. M. and Isaacs, H. V. (1996). eFGF, Xcad3 and Hox genes form a molecular pathway that establishes the anteroposterior axis in Xenopus. *Development* **122**, 3881-3892.
Rida, P. C., Le Minh, N. and Jiang, Y. J. (2004). A Notch feeling of somite segmentation and beyond. *Dev. Biol.* **265**, 2-22.
Rupp, R. A. and Weintraub, H. (1991). Ubiquitous MyoD transcription at the midblastula transition precedes induction-dependent MyoD expression in presumptive mesoderm of X. laevis. *Cell* **65**, 927-937.
Saga, Y. and Takeda, H. (2001). The making of the somite: molecular events in vertebrate segmentation. *Nat. Rev. Genet.* **2**, 835-845.
Saga, Y., Hata, N., Koseki, H. and Taketo, M. M. (1997). Mesp2: a novel mouse gene expressed in the presegmented mesoderm and essential for segmentation initiation. *Genes Dev.* **11**, 1827-1839.
Sawada, A., Fritz, A., Jiang, Y. J., Yamamoto, A., Yamasu, K., Kuroiwa, A., Saga, Y. and Takeda, H. (2000). Zebrafish Mesp family genes, mesp-a and mesp-b are segmentally expressed in the presomitic mesoderm, and Mesp-b confers the anterior identity to the developing somites. *Development* **127**, 1691-1702.
Sawada, A., Shinya, M., Jiang, Y. J., Kawakami, A., Kuroiwa, A. and Takeda, H. (2001). Fgf/MAPK signalling is a crucial positional cue in somite boundary formation. *Development* **128**, 4873-4880.
Sive, H. L., Grainger, R. M. and Harland, R. M. (2000). *Early Development of Xenopus laevis: A laboratory Manual*. New York: Cold Spring Harbor Laboratory Press.
Slack, J. M., Isaacs, H. V., Song, J., Durbin, L. and Pownall, M. E. (1996). The role of fibroblast growth factors in early Xenopus development. *Biochem. Soc. Symp.* **62**, 1-12.
Smith, J. C., Price, B. M., Green, J. B., Weigel, D. and Herrmann, B. G. (1991). Expression of a Xenopus homolog of Brachyury (T) is an immediate-early response to mesoderm induction. *Cell* **67**, 79-87.
Sparrow, D. B., Jen, W. C., Kotecha, S., Towers, N., Kintner, C. and Mohun, T. J. (1998). Thylacine 1 is expressed segmentally within the paraxial mesoderm of the Xenopus embryo and interacts with the Notch pathway. *Development* **125**, 2041-2051.
Sumanas, S., Strege, P., Heasman, J. and Ekker, S. C. (2000). The putative wnt receptor Xenopus frizzled-7 functions upstream of beta-catenin in vertebrate dorsoventral mesoderm patterning. *Development* **127**, 1981-1990.
Takahashi, Y., Koizumi, K., Takagi, A., Kitajima, S., Inoue, T., Koseki, H. and Saga, Y. (2000). Mesp2 initiates somite segmentation through the Notch signalling pathway. *Nat. Genet.* **25**, 390-396.
Wallingford, J. B. and Habas, R. (2005). The developmental biology of Dishevelled: an enigmatic protein governing cell fate and cell polarity. *Development* **132**, 4421-4436.
Wolda, S. L., Moody, C. J. and Moon, R. T. (1993). Overlapping expression of Xwnt-3A and Xwnt-1 in neural tissue of Xenopus laevis embryos. *Dev. Biol.* **155**, 46-57.
Yamamoto, A., Nagano, T., Takehara, S., Hibi, M. and Aizawa, S. (2005). Shisa promotes head formation through the inhibition of receptor protein maturation for the caudalizing factors, Wnt and FGF. *Cell* **120**, 223-235.
Yoon, J. K. and Wold, B. (2000). The bHLH regulator pMesogenin1 is required for maturation and segmentation of paraxial mesoderm. *Genes Dev.* **14**, 3204-3214.
Yoon, J. K., Moon, R. T. and Wold, B. (2000). The bHLH class protein pMesogenin1 can specify paraxial mesoderm phenotypes. *Dev. Biol.* **222**, 376-391.